Experimental and Theoretical Evidence for $U(C_6H_6)$ and $Th(C_6H_6)$ Complexes

Ivan Infante,[†] Juraj Raab,[†] Jonathan T. Lyon,[‡] Binyong Liang,[‡] Lester Andrews,[‡] and Laura Gagliardi*,[†]

Department of Physical Chemistry, University of Geneva, 30 Quai Ernest Ansermet, CH-1211 Geneva, Switzerland, and Department of Chemistry, University of Virginia, McCormick Road, Charlottesville, Virginia 22904-4319

Received: August 5, 2007; In Final Form: September 10, 2007

The vibrational spectra of UBz and ThBz have been measured in solid argon. Complementary quantum chemical calculations have allowed the assignments of the vibrational spectra. According to the calculations, AcBz are stable molecules, as well as other species like BzAcBz and $BzAc_2Bz$. Experimentally, there is no evidence for the sandwich compounds BzAcBz and $BzAc_2Bz$ due to the limitations in the reagent concentrations.

Actinide chemistry is fascinating because of the complex electronic structure of actinide atoms and their molecular compounds, but at the same time, it poses many challenges from both an experimental and computational perspective. Matrix isolation techniques, in combination with laser ablation, have been shown to be very powerful for the formation and characterization of novel chemical species.[1,2] High-level quantum chemical calculations allow the identification of the nature of the electronic states of such compounds. The multiple bond between two U atoms in the U_2 diatomic molecule, and in other earlier diactinides, Ac_2, Th_2, and Pa_2, has been recently investigated by *ab initio* quantum chemistry.[3,4] The U_2 dication, U_2^{2+}, has also been studied,[5] together with some possible molecules including the U_2 moiety, like PhUUPh,[6] and a number of diuranium polychlorides and polyformates.[7] Spectroscopic evidence was recently obtained for the novel complex, $UH_4(H_2)_6$,[8] which has potential interest as a metal hydride with a large number of hydrogen atoms bound to uranium. The calculations showed that the series of complexes $UH_4(H_2)_{1,2,4,6}$ are stable.

A considerable amount of work has been done on transition metal complexes with benzene, and these early investigations have been listed in recent work from the Virginia laboratory involving group 4 and 5 metal transition metal atoms.[9,10] The first experimental evidence for carbon ring deformation on complexation with group 4 metal atoms has recently been observed. The chemistry of actinide metal atoms often parallels that of their transition metal analogs. For example, similar metallocene species have been formed with both zirconium and thorium metals.[11−13] Hence, it is of interest to study benzene reactions with thorium and uranium metal atoms and compare the results to the analogous reactions with group 4 transition metals and chromium[14,15] in matrix environments. In these transition metal experiments, the lighter 3d metal atoms form sandwich $M(C_6H_6)_2$ complexes, whereas the heavier 4d and 5d transition metals form both $M(C_6H_6)$ and $M(C_6H_6)_2$ complexes. One of the goals of this study is to determine if actinide metal atoms react with benzene in condensing argon to form half-sandwich complexes, full-sandwich species, a combination of the two, or some higher order aggregate. Recently, gas-phase complexes $U^+(C_6H_6)_n$ have been produced by the combination of laser-ablated U^+ cations and benzene for the investigation of laser photodissociation.[16]

From a theoretical standpoint, determining the ground electronic states of $M(C_6H_6)$ complexes is not always a trivial task. For example, the lowest energy structures of $Ti(C_6H_6)$ have been reported as having spin multiplicities of 3 and 5, and $V(C_6H_6)$ has been reported in the doublet, quartet, and sextet states.[9,10] Matrix isolation has been shown to be an effective technique to trap these reaction intermediates, providing some experimental data for comparison to theory. Although neutral actinide $M(C_6H_6)$ species have not been reported either experimentally or theoretically to our knowledge, the full-sandwich $M(C_6H_6)_2$ complexes have been previously studied. Marcalo et al.[17] studied gas-phase reactions of M^+, M^{2+}, MO^+ (M = Th, U), and UO_2^+ with several arenes (benzene, naphthalene, toluene, mesitylene, hexamethylbenzene, and 1,3,5-tri-*tert*-butylbenzene) by Fourier transform ion cyclotron resonance mass spectrometry. Dolg et al.[18−20] theoretically investigated sandwich compounds of bis(benzene)lanthanide and actinide type. However, they focused more on the performance of different methods, rather than the chemical properties of these systems and they considered only linear isomers. The work by Li and Bursten,[21] on the other hand, explored different structures for the $M_2(C_6H_6)$ (M = Th, U) compounds and showed that these complexes prefer a bent structure rather a linear structure.

We here present the results of a combined experimental and theoretical study of the AcC_6H_6 (Ac = U, Th) complexes (from now indicated as AcBz). The BzAcBz and $BzAc_2Bz$ sandwich compounds were also considered theoretically. Several electronic states of various symmetries and spin multiplicities were investigated. The symmetry constraints were relaxed in most of the geometry optimizations, to find the global minimum for each species. Moreover, multiconfigurational calculations (see below) were performed to understand the nature of the electronic structure of these compounds. Experimentally, laser-ablated Th and U atoms were reacted in excess argon and infrared spectra were recorded. Measured vibrational frequencies were then compared with the calculated vibrational frequencies to assign the spectrum.

* Corresponding author. E-mail: laura.gagliardi@chiphy.unige.ch.
[†] University of Geneva.
[‡] University of Virginia.

10.1021/jp076279o CCC: $37.00
Published on Web 11/02/2007

Theoretical Methods

Quantum chemical calculations were performed using density functional theory (DFT) and multiconfigurational methods followed by second-order perturbation theory (CASSCF/CASPT2). The DFT calculations were performed using the TURBOMOLE package.[22] Scalar relativistic effects were incorporated by employing on the uranium and thorium atoms the (14s13p10d8f3g)/[10s9p5d4f3g] ECP basis set with 60 core electrons.[23] A TZVP valence triple-ζ basis set plus polarization function was used on the carbon atoms. The gradient-corrected BP86[24,25] exchange correlation functional was employed. Full geometry optimization and frequency calculations were performed for all species at the DFT/BP86 level of theory. Some calculations were also repeated with the PBE[26] and PBE0[27,28] functionals.

The CASSCF/CASPT2 calculations were performed only on the UBz and ThBz systems. The MOLCAS 6.7 program package[29] was employed. In the CASSCF/CASPT2 approach the complete active space CASSCF method[30] is used to generate wave functions for a predetermined set of electronic states. Dynamic correlation energy is added using second-order perturbation theory, CASPT2.[31] Scalar relativistic effects were included using a Douglas−Kroll−Hess Hamiltonian and relativistic ANO-RCC basis set[32] (4s3p2d1f for carbon, 2s1p for hydrogen, and 9s8p6d5f2g1h for uranium and thorium). In all the CASSCF/CASPT2 calculations C_{2v} symmetry was imposed.

In the CASSCF calculations the orbitals formed by linear combinations of 7s, 6d, and 5f orbitals of uranium/thorium with $2p_z$ orbitals of carbons (perpendicular to the Bz plane) were included in the active space, resulting in an active space formed of 12 electrons in 12 orbitals (12/12) for UBz and 10 electrons in 12 orbitals (10/12) for ThBz. In the following CASPT2 calculations, all orbitals up to and including 5d orbitals of uranium/thorium were kept frozen. Spin−orbit effects were estimated using the complete active space state interaction (CASSI) method, in which an effective one-electron spin−orbit Hamiltonian based on the atomic mean field approximation of the two-electron part is employed.[33] All CASSCF wave functions of the appropriate symmetries are used as basis functions to set up the SO Hamiltonian, and CASPT2 energies are used in the diagonal elements. This approach has been shown to work successfully in a number of earlier applications.[33−37] In the present calculation, the roots of all states (of all possible spins and symmetries) lying up to 0.65 eV (15 kcal/mol) from the lowest state were selected.

The fragment approach[38] as implemented in the ADF package[39] has been used to study the nature of the interaction between U/Th and Bz in UBz and ThBz. In this method, the bonding energy between two fragments is expressed as the sum of two terms, one destabilizing term called strain energy, and one stabilizing term called interaction energy: $\Delta E^{\text{bond}} = \Delta E^{\text{strain}} + \Delta E^{\text{int}}$. The ΔE^{strain} term is associated with the deformation of the individual fragments when they form the supersystem. This contribution is always positive and its magnitude depends on the rigidity and reorganization of each fragment. The ΔE^{int} term is the effective interaction between the deformed fragments. In our analysis the two subsystems are U/Th and the Bz ring.

Experimental Methods

Laser-ablated Th and U atoms were reacted with benzene and its deuterium (99.6%) and carbon-13 (99%) isotopic modifications (Cambridge Isotopic Laboratories) in excess argon (0.5% concentrations) during condensation onto an 8 K cesium iodide window as described previously.[40,41] Infrared spectra were recorded on a Nicolet 550 spectrometer after sample deposition, after annealing, and after irradiation using a 175 W mercury arc street lamp and selected optical filters.

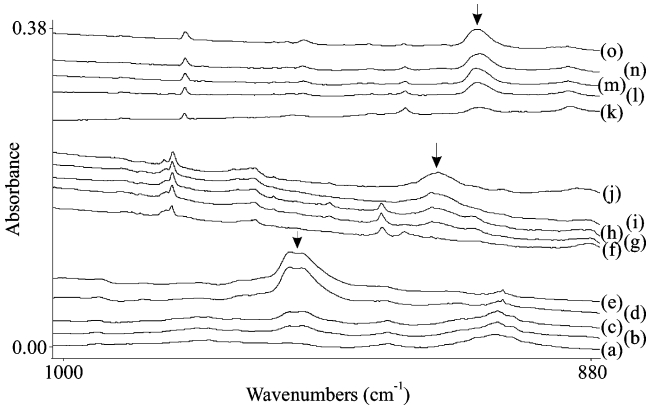

Figure 1. IR Spectra in the 1000−880 cm^{-1} region from co-depositing laser-ablated uranium atoms with (a) C_6H_6, (f) $^{13}C_6H_6$, and (k) C_6D_6 diluted to 0.5% in argon for 1 h at 8 K, and after the resulting samples were subjected to (b,g,l) annealing to 30 K, (c,h,m) annealing to 35 K, (d,i,n) full-arc (>220 nm) irradiation, and (e,j,o) annealing to 40K.

Results and Discussion

Experimental spectra and theoretical calculations will be presented for actinide metal-benzene complexes.

Matrix Infrared Spectra. ***Uranium and Benzene.*** Uranium atoms codeposited with benzene in excess argon gave a weak new absorption at 946.9 cm^{-1}. Annealing the sample to 25 K increased this absorption substantially and a second annealing to 30 K produced more growth. Next irradiation with the full light of the mercury arc lamp increased this absorption threefold and resolved subpeaks at 948.5 and 945.1 cm^{-1}. A final annealing to 40 K had little effect on the spectrum. Similar annealing and photochemical behavior was found for a new 914.9 cm^{-1} absorption with the carbon-13 and for a new 905.4 cm^{-1} band with the deuterium isotopic samples. Infrared spectra are compared for these isotopic samples in Figure 1. The ultraviolet irradiation that increased the 946.9 cm^{-1} absorption 3-fold markedly increased a shoulder at 680 cm^{-1} on the blue side of the very strong benzene band at 675 cm^{-1}, and this new absorption is 10-fold stronger than the 946.9 cm^{-1} band. Similar shoulders were observed at 677 and 500 cm^{-1} on the strong carbon-13 and deuterated benzene absorptions at 672 and 497 cm^{-1}. No other associated product absorptions were observed here, and none could be resolved from the unreacted benzene absorptions. We observed no product absorptions in the 600 cm^{-1} region below the strong benzene band. Finally, weak UO and UO_2 absorptions at 819.5 and 776.0 cm^{-1} are characteristic of uranium experiments as surface uranium oxides are ablated from the uranium target.[42]

Thorium and Benzene. Thorium atoms and benzene gave different new absorptions at 952.1 and 941.2 cm^{-1}, which increased on annealing and slightly on ultraviolet irradiation, as shown in Figure 2. Unlike uranium and benzene, no product absorption was observed on the blue side of the strong 675 cm^{-1} benzene band. The new product bands shifted to 918.9 and 907.2 cm^{-1} with carbon-13 and to 912.4 and 902.3 cm^{-1} with deuterium substitution. There was no evidence for thorium hydride absorptions, but weak thorium oxide bands were observed at 876.4 and 736.6 cm^{-1} (ref 43 and references therein).

Calculated Structures and Spectra. ***Uranium and Benzene.*** Calculations at the DFT/BP86 level predict the UBz system to have a $^5A_1$ ground state, in which the benzene ring is slightly

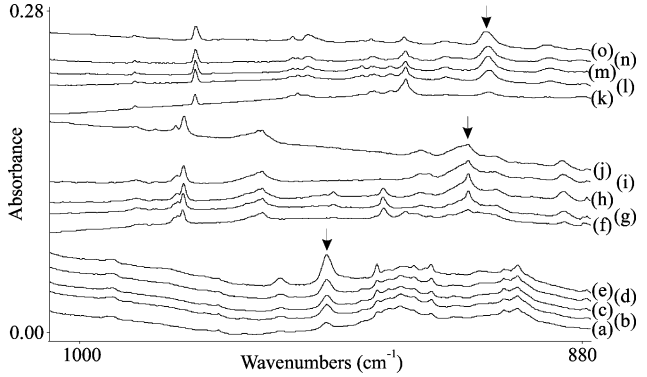

Figure 2. IR Spectra in the 1000−880 cm^{-1} region from co-depositing laser-ablated thorium atoms with (a) C_6H_6, (f) $^{13}C_6H_6$, and (k) C_6D_6 diluted to 0.5% in argon for 1 h at 8 K, and after the resulting samples were subjected to (b,g,l) annealing to 30 K, (c,h,m) annealing to 35 K, (d,i,n) full-arc(>220 nm) irradiation, and (e,j,o) annealing to 40K.

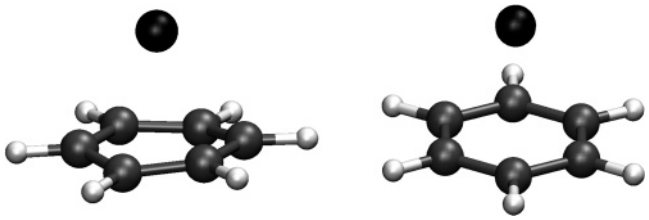

Figure 3. The structure of UBz, with the benzene ring slightly distorted from planarity and with the benzene ring planar.

distorted from planarity (Figure 3). The typical bond distances are reported in Table 1. The energy difference between the $^5A_1$ state and the $^7A_1$ state is of 0.09 kcal/mol ($^7A_1$ higher) at the DFT/BP86 level of theory. DFT calculations with the PBE and PBE0 functionals, respectively, predict the $^5A_1$ state to lie 2.01 kcal/mol lower in energy than the $^7A_1$ state and 1.3 kcal/mol higher in energy than the $^7A_1$ state, respectively. The $^7A_1$ state is predicted to be planar with all functionals, and the $^5A_1$ state is slightly distorted from planarity in all cases (see Table 1). In summary, all DFT calculations indicate that the two states lie close in energy. Moreover, other quintet and septet states, belonging to different irreducible representations, lie within 2−3 kcal/mol from the totally symmetric quintets and septets, confirming that there is a high density of states.

Multiconfigurational CASSCF/CASPT2 calculations were thus performed, and they predicted the ground state of UBz to be a $^7A_1$ (C_{2v} symmetry) with a planar benzene ring (Figure 3). The lowest quintet state, $^5A_1$, presents the benzene ring distorted, and it lies about 12 kcal/mol higher in energy than the ground state. This excitation energy is significantly larger than the value obtained at the DFT level (2 kcal/mol). The CASSCF wave function of the ground state of UBz is essentially single configurational, corresponding to six singly occupied orbitals, which are a linear combination of C $2p_z$ orbitals and U 7s, 6d, and 5f orbitals. The calculation including spin−orbit effects showed that the ground state is mainly composed of septet states, and the first state with a significant quintet contribution lies about 8 kcal/mol higher in energy than the ground state.

The calculated BP86 vibrational frequencies for the $^7A_1$ state of UBz are reported in Table 2, together with the observed values. In Tables SI1 and SI2 of the Supporting Information the normal modes for several other electronic states are reported. All the septet states have similar vibrational frequencies, and the same holds for the quintet states. We will thus focus on the analysis of the spectrum of the $^7A_1$ state (Table 2). The most intense observed peak in the spectrum is the out-of-plane C−H bending mode, ν_{o-p}(CH), occurring at 675 cm^{-1}. The calculated BP86 value is 673 cm^{-1}, for the $^7A_1$ state, and the same vibration for the $^5A_1$ is calculated at 719 cm^{-1}. The PBE functional predicts this mode at 674 and 718 cm^{-1}, respectively, for the $^7A_1$ state and the $^5A_1$ state, respectively. The experimental H/D ratio for this mode is 1.358 (Table SI3). This value is well reproduced by the BP86 calculated septet H/D ratio, 1.335, but the BP86 calculated quintet H/D ratio is only 1.292. The breathing mode, ν_s(CC), is observed at 947 cm^{-1}. The computed vibrational frequency for the septet state is 938 cm^{-1}, and for the quintet state it is 911 cm^{-1}. The H/D ratios calculated at the BP86 level for the septet and quintet states are 1.047 and 1.032, respectively. Also in this case, the calculated value for the septet matches better the experimental value. This comparison between the observed and calculated spectra seems to indicate that the observed spectrum corresponds to the $^7A_1$ state rather than the $^5A_1$ state.

The bands computed at 972 and 975 cm^{-1}, with an intensity of 10 km/mol were not observed experimentally. One should, however, bear in mind that intensities are very difficult to predict from calculations. Furthermore, many product bands are not shifted away from the benzene parent and cannot be observed here. In view of these considerations, the agreement between experiment and theory is remarkably solid.

Other possible species, eventually present in the matrix, like the sandwich compounds BzUBz, and BzU_2Bz, were also considered (Figure 4a,b). Several spin states were explored. Their structures were optimized and their vibrational spectra were computed. The relevant information is reported in the Supporting Information (Tables SI4−SI7). Possible formation reactions were considered for the various species. The energy differences between the various species, including zero-point energy corrections are reported in Table 3. The formation of UBz from U and Bz is exothermic, as is the formation of BzUBz and BzU_2Bz. Moreover, according to the calculations, BzU_2Bz is more stable than two UBz, but there is no experimental evidence of such sandwich species. A comparison of the results obtained with the different functionals (Table 3) shows that, for the reactions involving UBz and UBz_2, BP86 and PBE0 give similar results, and PBE generally predicts lower energy differences, whereas for the reactions involving BzU_2Bz and for the formation of U_2 from 2U, BP86 agrees better with PBE, rather than PBE0. The value of 29 kcal/mol as an energy difference between U_2 and 2 U atoms obtained at the PBE0 level is in agreement with what we previously obtained at the CASPT2 level of theory,[3] namely, 23 kcal/mol.

Thorium and Benzene. DFT predicts ThBz to have a triplet ^3A ground state. The lowest singlet state, ^1A, lies 6.5, 5.3, and 7.1 kcal/mol higher in energy than the ^3A state, at the BP86, PBE, and PBE0 level of theory, respectively. The typical bond distances are reported in Table 4. CASSCF/CASPT2, on the other hand, predicts the lowest singlet to lie only 0.5 kcal/mol above the ground state. The CASSCF wave function of the $^3A_1$ state (in C_{2v} symmetry) is single configurational and corresponds to two singly occupied orbitals, which are a linear combination of C $2p_z$ and Th 7s and 6d orbitals. Inclusion of spin−orbit coupling shows that the lowest state is mainly composed of the spin-free $^3A_1$ state and the first excited state lying 1.5 kcal/mol above the ground state is mainly composed of the $^1A_1$ state.

The calculated and observed vibrational frequencies for ThBz are reported in Table 5. In analogy with what was already done for U, other possible species, eventually present in the matrices, like BzThBz and $BzTh_2Bz$, were also considered (the relevant information is reported in the Supporting Information, Tables

TABLE 1: Structural Parameters of UBz Calculated at Various Levels of Theory[a]

	CASPT2 $^7A_1$	BP86 $^7A_1$	BP86 $^5A_1$	PBE $^7A_1$	PBE $^5A_1$	PBE0 $^7A_1$	PBE0 $^5A_1$
R(U−C)/Å	2.61	2.66	2.53/2.61	2.66	2.45/2.65	2.64	2.45/2.69
R(C−C)/Å	1.40	1.42	1.42/1.46	1.42	1.38/1.46	1.41	1.36/1.46
R(C−H)/Å	1.08	1.08	1.09	1.09	1.09	1.08	1.08
dist, deg	0	0	12	0	12	0	13

[a] The distortion (dist) indicates how much the benzene ring is distorted from planarity.

TABLE 2: Observed and Calculated (DFT/BP86/TZVP Level of Theory) Isotopic Frequencies (cm^{-1}) and Intensities (km/mol) for the $^7A_1$ State of UBz[a]

			C_6H_6			C_6D_6			$^{13}C_6H_6$		
irrep	species	mode	obs	calc	int	obs	calc	int	obs	calc	int
a_1	UBz	ν_a(MC)		242	1		231	0.1		235	1
a_1		ν_{o-p}(CH)	675	673	111	497	504	54	672	670	92
b_1		ν_{o-p}(CH)		737	1		571	0.2		731	1
b_2		ν_{o-p}(CH)		738	2		574	0.2		733	2
a_1		ν_s(CC)	947	938	8	905	896	9	915	905	8
b_1		ν_{i-p}(CH)		972	10		773	7		951	8
b_2		ν_{i-p}(CH)		975	10		774	7		954	10
b_1		ν_a(CC)		1408	2		1246	0.2		1383	2
b_2		ν_a(CC)		1411	2		1350	0.2		1386	2

[a] The calculations have been performed imposing C_{2v} symmetry.

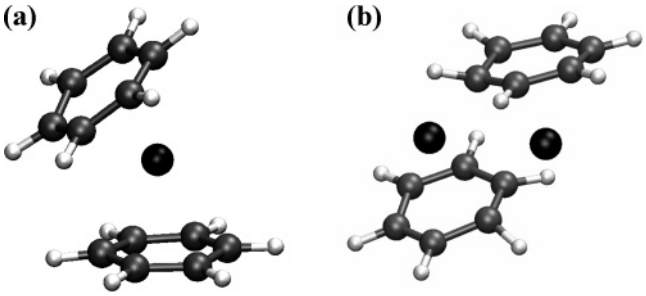

Figure 4. (a) The structure of BzUBz. (b) The structure of BzUUBz

TABLE 3: Energy Differences (kcal/mol) between Various UBz Species, in Their Lowest Electronic State[a]

	BP86	PBE	PBE0
E(UBz) − (E(U) + E(Bz))	−45(−46)	−12	−45
E(UBz$_2$) − (E(U) + 2E(Bz))	−92(−95)	−30	−87
E(U$_2$Bz$_2$) − 2(E(U) + E(Bz))	−174(−177)	−120	−139
E(U$_2$Bz$_2$) − 2E(UBz)	−89(−82)	−96	−49
E(U$_2$) − 2E(U)	−70(−70)	−75	−29

[a] The values including zero point energy corrections are reported in parentheses. The following electronic states were considered: UBz $^7A_1$ in C_{2v}; UBz$_2$ ^5A in C_1; U$_2$Bz$_2$ ^5A in C_1; U$_2$ $^7E_{2g}$ in D_{6h}; U ^5L.

TABLE 4: Structural Parameters of ThBz.

	CASPT2 $^3A_1$	BP86 $^3A_1$	BPE $^3A_1$	PBE0 $^3A_1$
R(Th−C)/Å	2.58/2.61	2.47/2.62	2.46/2.61	2.44/2.59
R(C−C)/Å	1.40/1.42	1.40/1.46	1.42/1.46	1.41/1.45
R(C−H)/Å	1.08	1.09	1.09	1.08

SI8−SI11). The energy differences between the various species, including zero-point energy corrections are reported in Table 6. The formation reactions for ThBz, BzThBz, and BzTh$_2$Bz are all exothermic. As already noticed in the U case, BP86 and PBE0 give similar results for all the reactions involving Th and Bz, whereas for the formation reaction of Th$_2$ from two Th atoms, there is a better agreement between BP86 and PBE. All three DFT calculations predict Th$_2$ to have a dissociation energy of 86−97 kcal/mol, but our previous CASPT2 calculation[3] predicted a dissociation energy of only 65 kcal/mol.

TABLE 5: Observed and Calculated (DFT/BP86/TZVP Level of Theory) Isotopic Frequencies (cm^{-1}) and Intensities (km/mol) for ThBz[a]

		C_6H_6			C_6D_6			$^{13}C_6H_6$		
sym	mode	obs	calc	int	obs	calc	int	obs	calc	int
a	ν_a(MC)		264	6		244	8		257	5
a	ν_{o-p}(CC)		391	10		353	7		379	9
a	ν_{o-p}(CC)		514	6		465	0.3		497	6
b	ν_{o-p}(CC)		524	1		464	2		506	1
b	ν_{o-p}(CH)		657	6		502	2		653	6
a	ν_{o-p}(CH)		698	17		541	9		693	3
b	ν_{o-p}(CH)		706	2		554	1		701	2
a	ν_{o-p}(CH)		709	74		542	32		702	89
b	ν_{o-p}(CH)		828	1		761	4		822	2
a	ν_s(CC)	947	911	14	902	877	3	907	879	12
b	ν_{i-p}(CH)		913	23		742	15		891	22
b	ν_{i-p}(CH)		964	7		877	16		943	6
a	ν_a(CC)		1123	3		994	0		1117	2
b	ν_a(CC)		1305	13		1192	2		1267	16
b	ν_a(CC)		1436	10		1392	22		1395	6
a	ν_a(CC)		1479	6		1439	8		1429	5

[a] All calculations have been performed imposing C_2 symmetry.

TABLE 6: Energy Differences (kcal/mol) between Various ThBz Species, in Their Lowest Electronic State[a]

	BP86	PBE	PBE0
E(ThBz) − (E(Th) + E(Bz))	−60(−62)	−30	−62
E(ThBz$_2$) − (E(Th) + 2E(Bz))	−105(−107)	−43	−110
E(Th$_2$Bz$_2$) − 2(E(Th) + E(Bz))	−186(−190)	−131	−187
E(Th$_2$Bz$_2$) − 2E(ThBz)	−66(−66)	−71	−63
E(Th$_2$) − 2E(Th)	−92(−92)	−97	−86

[a] The values including zero point energy corrections are reported in parentheses. The following electronic states were considered: ThBz ^3A in C_2; ThBz$_2$ ^1A in C_1; Th$_2$Bz$_2$ ^1A in C_1; Th$_2$ $^3A_{2u}$ in D_{6h}; Th ^3F.

Bond Analysis. In UBz, the energy of deformation of the benzene ring is only 2 kcal/mol, indicating a marginal rearrangement. The total strain energy is about 42 kcal/mol, and it includes the rearrangement due to the change of spin multiplicity of uranium. It is compensated by the interaction energy, which has opposite sign, of about 81 kcal/mol. A closer inspection of this term indicates that the electrons move in both directions, with π donation from the HOMO and HOMO−1 orbitals of the benzene ring to the 5fπ and 6dπ orbitals of uranium, and

with σ back-donation from the 7s, 5fσ, 6dσ, and a small contribution also from the δ orbitals, to the empty LUMO and LUMO+1 orbitals of benzene. The overall transfer of electrons is 0.17 from the uranium atom to the benzene ring. The total binding energy is 40 kcal/mol.

In ThBz, the energy of the out of plane deformation of the benzene ring is 10 kcal/mol, which is larger than in UBz. The orbital energy contribution is similar to the uranium case. The charge transfer between Th and Bz is slightly lower than between U and Bz. This suggests that the main reason why ThBz has a larger bonding energy than UBz is that uranium undergoes a change in spin-multiplicity due to its interaction with benzene, but Th does not. According to the CASSCF/CASPT2 calculations the total dipole moment of ThBz is 0.7 debye, and the total dipole moment of UBz is only 0.2 debye. DFT also predicts similar dipole moments. Inspection of the molecular orbitals involved in the bonding between the metal and the Bz ring indicates that the extra electrons in U not present in Th are back-donated to the Bz ring, making UBz less polar than ThBz.

Conclusions

The results of a combined experimental and computational study of AcBz (Ac = U and Th) have been reported. According to the calculations, AcBz are stable molecules, as well as other species like BzAcBz and $BzAc_2Bz$. Vibrational bands for U/Th and Bz systems have been measured in an argon matrix and have been assigned to the UBz and ThBz species. Experimentally, there is no evidence for the sandwich compounds BzAcBz and $BzAc_2Bz$ due to the limitations in the reagent concentrations.

Acknowledgment. This work was supported by the Swiss National Science Foundation (grant no. 200021-111645/1) and the U.S. National Science Foundation (Grant CHE 03-52487).

Supporting Information Available: Tables with structural parameters, vibrational frequencies and intensities, and isotopic ratios for some AcBz, $AcBz_2$, and Ac_2Bz_2 species (Ac = U, Th). This material is available free of charge via the Internet at http://pubs.acs.org.

References and Notes

(1) Andrews, L. *Chem. Soc. Rev.* **2004**, *33*, 123.
(2) Zhou, M. F.; Andrews, L.; Li, J.; Bursten, B. E. *J. Am. Chem. Soc.* **1999**, *121*, 9712.
(3) Roos, B. O.; Malmqvist, P. A.; Gagliardi, L. *J. Am. Chem. Soc.* **2006**, *128*, 17000.
(4) Gagliardi, L.; Roos, B. O. *Nature* **2005**, *433*, 848.
(5) Gagliardi, L.; Pyykko, P.; Roos, B. O. *Phys. Chem. Chem. Phys.* **2005**, *7*, 2415.
(6) La Macchia, G.; Brynda, M.; Gagliardi, L. *Angew. Chem., Int. Ed.* **2006**, *45*, 6210.
(7) Roos, B. O.; Gagliardi, L. *Inorg. Chem.* **2006**, *45*, 803.
(8) Raab, J.; Lindh, R. H.; Wang, X.; Andrews, L.; Gagliardi, L. *J. Phys. Chem. A* **2007**, *111*, 6383.
(9) Lyon, J. T.; Andrews, L. *J. Phys. Chem. A* **2005**, *109*, 431.
(10) Lyon, J. T.; Andrews, L. *J. Phys. Chem. A* **2006**, *110*, 7806.
(11) Yang, X. M.; King, W. A.; Sabat, M.; Marks, T. J. *Organometallics* **1993**, *12*, 4254.
(12) Hlatky, G. G.; Eckman, R. R.; Turner, H. W. *Organometallics* **1992**, *11*, 1413.
(13) Chen, E. Y. X.; Marks, T. J. *Chem. Rev.* **2000**, *100*, 1391.
(14) Boyd, J. W.; Lavoie, J. M.; Gruen, D. M. *J. Chem. Phys.* **1974**, *60*, 4088.
(15) Efner, H. F.; Tevault, D. E.; Fox, W. B.; Smardzewski, R. R. *J. Organomet. Chem.* **1978**, *146*, 45.
(16) Pillai, E. D.; Molek, K. S.; Duncan, M. A. *Chem. Phys. Lett.* **2005**, *405*, 247.
(17) Marcalo, J.; Leal, J. P.; deMatos, A. P.; Marshall, A. G. *Organometallics* **1997**, *16*, 4581.
(18) Dolg, M. *J. Chem. Inf. Comput. Sci.* **2001**, *41*, 18.
(19) Hong, G. Y.; Schautz, F.; Dolg, M. *J. Am. Chem. Soc.* **1999**, *121*, 1502.
(20) Hong, G. Y.; Dolg, M.; Li, L. M. *Int. J. Quantum Chem.* **2000**, *80*, 201.
(21) Li, J.; Bursten, B. E. *J. Am. Chem. Soc.* **1999**, *121*, 10243.
(22) Ahlrichs, R.; Bar, M.; Haser, M.; Horn, H.; Kolmel, C. *Chem. Phys. Lett.* **1989**, *162*, 165.
(23) Cao, X. Y.; Dolg, M. *J. Mol. Struct. (THEOCHEM)* **2004**, *673*, 203.
(24) Becke, A. D. *Phys. Rev. A* **1988**, *38*, 3098.
(25) Perdew, J. P. *Phys. Rev. B* **1986**, *33*, 8822.
(26) Perdew, J. P.; Burke, K.; Ernzerhof, M. *Phys. Rev. Lett.* **1996**, *77*, 3865.
(27) Adamo, C.; Barone, V. *J. Chem. Phys.* **1999**, *110*, 6158.
(28) Ernzerhof, M.; Scuseria, G. E. *J. Chem. Phys.* **1999**, *110*, 5029.
(29) Karlstrom, G.; Lindh, R.; Malmqvist, P. A.; Roos, B. O.; Ryde, U.; Veryazov, V.; Widmark, P. O.; Cossi, M.; Schimmelpfennig, B.; Neogrady, P.; Seijo, L. *Comput. Mater. Sci.* **2003**, *28*, 222.
(30) Roos, B. O.; Taylor, P. R.; Siegbahn, P. E. M. *Chem. Phys.* **1980**, *48*, 157.
(31) Andersson, K.; Malmqvist, P. A.; Roos, B. O. *J. Chem. Phys.* **1992**, *96*, 1218.
(32) Roos, B. O.; Lindh, R.; Malmqvist, P. A.; Veryazov, V.; Widmark, P. O. *Chem. Phys. Lett.* **2005**, *409*, 295.
(33) Roos, B. O.; Malmqvist, P. A. *Phys. Chem. Chem. Phys.* **2004**, *6*, 2919.
(34) Gagliardi, L.; Heaven, M. C.; Krogh, J. W.; Roos, B. O. *J. Am. Chem. Soc.* **2005**, *127*, 86.
(35) Roos, B. O.; Widmark, P. O.; Gagliardi, L. *Faraday Discuss.* **2003**, *124*, 57.
(36) Gagliardi, L.; La Manna, G.; Roos, B. O. *Faraday Discuss.* **2003**, *124*, 63.
(37) Gagliardi, L. *Theor. Chem. Acc.* **2006**, *116*, 307.
(38) Bickelhaupt, F. M.; Baerends, E. J. *Rev. Comput. Chem.* **2000**, *15*, 1.
(39) Fonseca Guerra, C.; Snijders, J. G.; te Velde, G.; Baerends, E. J. *Theor. Chem. Acc.* **1998**, *99*, 391.
(40) Lyon, J. T.; Andrews, L. *Inorg. Chem.* **2006**, *45*, 1847.
(41) Lyon, J. T.; Andrews, L. *Inorg. Chem.* **2005**, *44*, 8610.
(42) Hunt, R. D.; Yustein, J. T.; Andrews, L. *J. Chem. Phys.* **1993**, *98*, 6070.
(43) Souter, P. F.; Kushto, G. P.; Andrews, L.; Neurock, M. *J. Phys. Chem. A* **1997**, *101*, 1287.